the plant journal

SEB Society for Experimental Biology

The Plant Journal (2015) **83,** 831–844 doi: 10.1111/tpj.12930

Functional characterization of mutants affected in the carbonic anhydrase domain of the respiratory complex I in *Arabidopsis thaliana*

Débora Soto[1], Juan Pablo Córdoba[1], Fernando Villarreal[1], Carlos Bartoli[2], Jessica Schmitz[3], Veronica G. Maurino[3], Hans Peter Braun[4], Gabriela C. Pagnussat[1] and Eduardo Zabaleta[1,*]

[1]*Instituto de Investigaciones Biológicas IIB/CONICET, Universidad Nacional de Mar del Plata, cc 1245, 7600 Mar del Plata, Argentina,*

[2]*Instituto de Fisiología Vegetal, Universidad Nacional de La Plata/CONICET La Plata, cc 327, 1900 La Plata, Argentina,*

[3]*Plant Molecular Physiology and Biotechnology Group, Institute of Developmental and Molecular Biology of Plants, Cluster of Excellence on Plant Sciences, Heinrich Heine Universität, Universitätsstraße 1, 40225 Düsseldorf, Germany, and*

[4]*Institute for Plant Genetics, Leibniz Universität Hannover, Herrenhäuserstraße 2, D–30419 Hannover, Germany*

Received 18 February 2015; revised 16 June 2015; accepted 17 June 2015; published online 3 July 2015.
*For correspondence (e-mail ezabalet@mdp.edu.ar).

SUMMARY

The NADH–ubiquinone oxidoreductase complex (complex I) (EC 1.6.5.3) is the main entrance site of electrons into the respiratory chain. In a variety of eukaryotic organisms, except animals and fungi (Opisthokonta), it contains an extra domain comprising trimers of putative γ–carbonic anhydrases, named the CA domain, which has been proposed to be essential for assembly of complex I. However, its physiological role in plants is not fully understood. Here, we report that Arabidopsis mutants defective in two CA subunits show an altered photorespiratory phenotype. Mutants grown in ambient air show growth retardation compared to wild–type plants, a feature that is reversed by cultivating plants in a high-CO_2 atmosphere. Moreover, under photorespiratory conditions, carbon assimilation is diminished and glycine accumulates, suggesting an imbalance with respect to photorespiration. Additionally, transcript levels of specific CA subunits are reduced in plants grown under non-photorespiratory conditions. Taken together, these results suggest that the CA domain of plant complex I contributes to sustaining efficient photosynthesis under ambient (photorespiratory) conditions.

Keywords: ***Arabidopsis thaliana*, γ–carbonic anhydrases, mitochondria, photorespiration, carbon recycling.**

INTRODUCTION

The NADH–ubiquinone oxidoreductase (complex I, CI) (EC 1.6.5.3) is the largest complex of the mitochondrial or bacterial respiratory chain. It catalyzes the transfer of two electrons from NADH to quinone, coupled with proton translocation across the membrane. In many systems, it represents the major entry point of electrons from metabolic reactions (Gray, 2012).

The bacterial CI is made up of 14 subunits. Two of these are fused in *Escherichia coli*, resulting in a 13-subunit enzyme, which represents the core complex (Friedrich, 1998). Eukaryotic CI contains an additional 31-38 so-called 'accessory subunits', with the number differing among species (Bridges *et al.*, 2010; Cardol, 2011; Andrews *et al.*, 2013; Peters *et al.*, 2013; Braun *et al.*, 2014). Using single-particle electron microscope analysis of isolated CI from Arabidopsis and *Polytomella* spp, a specific matrix-exposed domain formed by γ–carbonic anhydrase (CA) subunits attached to the membrane arm of the complex was identified (Dudkina *et al.*, 2005; Sunderhaus *et al.*, 2006). This domain is absent in CI from animals (Andrews *et al.*, 2013). In Arabidopsis, this protein domain contains at least two different γ–CA proteins, CA1 (At1g19580) and CA2 (At1g47260), which show conserved active-site regions, and two less well-conserved γ–CA-like proteins, CAL1 (At5g63510) and CAL2 (At3g48680), containing non-conservative replacements of putatively important amino acids (Parisi *et al.*, 2004; Perales *et al.*, 2004). It was proposed that the CA domain is formed by trimers comprising two CA subunits and one CAL subunit, probably varying among individual CI particles (Perales *et al.*, 2005; Zabaleta *et al.*, 2012). Further investigations failed to identify a third CA protein (CA3, At5g66510) within the CA domain,

although it was shown to represent a CI subunit (Klodmann *et al.*, 2010; Peters *et al.*, 2013; Braun *et al.*, 2014).

The γ–CA subunits were first thought to be specific to CI from photosynthetic organisms (Heazlewood *et al.*, 2003; Parisi *et al.*, 2004). However, further investigations demonstrated that homologous γ–CA proteins also exist in CI isolated from *Euglena* spp (Perez *et al.*, 2014). More intriguing is the discovery of these subunits in CI from slime moulds (*Dictyostelium* spp) and amoebae (*Acanthamoeba* spp) that lack photosynthesis (Gawryluk and Gray, 2010). Homologous sequences were also reported in a range of other eukaryotic lineages (Gawryluk and Gray, 2010). Up to now, γ–CA proteins have not been found in animals and fungi. A role in CI assembly has been postulated (Perales *et al.*, 2005) and experimentally proved in several independent experiments (Klodmann *et al.*, 2010; Meyer *et al.*, 2011; Li *et al.*, 2013). Furthermore, specific roles of γ–CA proteins in photomorphogenesis in plants have been demonstrated (Wang *et al.*, 2012) and male reproductive development by overexpression of one of the subunits (Villarreal *et al.*, 2009).

Recently, a link of γ–CAs to photorespiration was also postulated (Braun and Zabaleta, 2007; Zabaleta *et al.*, 2012). Ribulose bisphosphate carboxylase/oxygenase (Rubisco) has two activities that use the same active site: a carboxylase, which is needed to sustain plant growth, and an oxygenase, leading to the synthesis of the toxic 2–phosphoglycolate (2-PG) in chloroplasts. Accumulation of 2–PG leads to inhibition of metabolic processes that impair CO_2 assimilation. Highly toxic metabolic effects of 2–PG accumulation were demonstrated *in planta* using a glycolate oxidase (GOX) loss-of-function mutant (*go1*) of the C4 species maize (*Zea mays*) (Zelitch *et al.*, 2009). Oxygenic autotrophs evolved the photorespiratory pathway to detoxify 2–PG by recycling assimilated carbon (Maurino and Peterhänsel, 2010). In this pathway, 2–PG is converted to glycolate, which is further catabolized in the peroxisomes, producing hydrogen peroxide and glycine by the actions of GOX (Esser *et al.*, 2014) and glutamate-glyoxylate amino transferase (GGAT) (Maurino and Peterhänsel, 2010). Glycine is further transported to mitochondria, where it is decarboxylated through the action of glycine decarboxylase (GDC) and converted into serine by serine hydroxymethyl transferase (SHMT) (Maurino and Peterhänsel, 2010). The serine produced by this reaction is transported back to the peroxisome for further metabolism, and the concomitant CO_2 is liberated. However, carbon assimilation studies indicate that not all the CO_2 produced is lost, suggesting that a proportion of carbon is being recycled (Bauwe *et al.*, 2010; Zabaleta *et al.*, 2012). It has been proposed (in *Chlamydomonas reinhardtii* as well as in plants) that carbon in the form of bicarbonate is exported through a putative transporter of inorganic carbon (HCO_3^- and CO_2) in the mitochondrial membrane (Raven, 2001; Riazunnisa *et al.*, 2006; Zabaleta *et al.*, 2012). Although carbonic anhydrase activity of the CA domain has not been experimentally confirmed, one of the CA subunits (CA2 protein) is able to bind inorganic carbon in a specific manner (Martin *et al.*, 2009). Accordingly, it has been postulated that the CA domain may represent this elusive inorganic carbon transporter of the mitochondrial membrane that may be involved in recycling CO_2 from respiration and photorespiration (Braun and Zabaleta, 2007, Zabaleta *et al.*, 2012).

Here, we present experimental evidence that the CA domain of plant CI is involved in carbon metabolism. Mutants affected simultaneously in two CA subunits display an altered photorespiratory phenotype; the plants show growth retardation in normal air but develop like wild-type under high-CO_2 (non-photorespiratory) conditions. In addition, under photorespiratory conditions, carbon assimilation is compromised, production of reactive oxygen species (ROS) increases, and glycine accumulates.

RESULTS

Arabidopsis double mutants affected in specific subunits of the CA domain show growth retardation under ambient air

In order to investigate the physiological role of the CA domain of Arabidopsis CI, we used a reverse-genetics approach. As none of the single mutants for each of the genes encoding CA proteins (*ca1*, *ca2*, *ca3*, *cal1* or *cal2*) show an altered phenotype under ambient conditions (Figure 1a,b) (Perales *et al.*, 2005; Wang *et al.*, 2012), we performed crosses of single mutants to obtain various double mutant combinations that are affected in more than one subunit of this domain. Forty of the progeny plants were genotyped to identify at least two double mutant individuals for each cross, *ca2cal1* and *ca2cal2* (Figure 1a). While the double mutant *ca2cal1* is a double knockout mutant, the double mutant *ca2cal2* is a knockout mutant for the *CA2* gene and a knockdown mutant for the *CAL2* gene (Figure S1). All plants germinate normally in normal air (380 ppm of CO_2) under a short-day photoperiod (12 h light/12 h dark). However, after 10 days of growth, both double mutant lines begin to show significant retardation of growth. As the plants grow, this difference in size is maintained. By comparing the fifth leaf of 4-week-old plants, it may be observed that leaves of double mutants are consistently smaller than those of the wild-type (WT) or the single mutants (Figure 1b,c). Measurements of fresh and dry weights clearly show that double mutants are significantly lighter than WT plants (Figure 1d,e). Roots of the double mutants are smaller than those of the WT, and their flowering time is retarded when exposed to an inductive photoperiod (3.7 ± 0.5 days after WT flowering, $P \leq 0.05$) as has been shown for *cal1 cal2* RNAi plants (Wang *et al.*, 2012).

As none of the single mutants grown under short-day conditions showed an altered phenotype, introducing a wild-

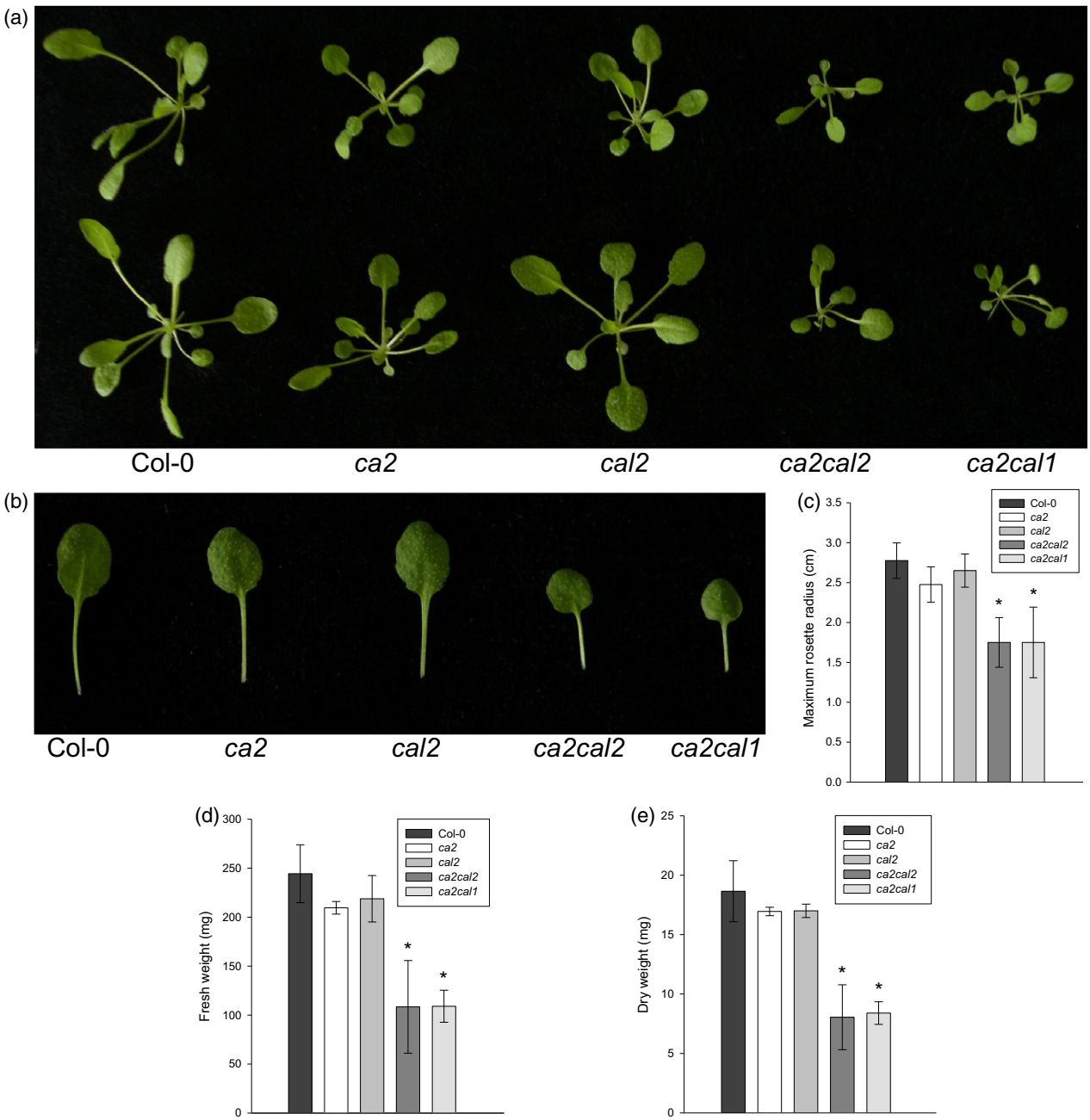

Figure 1. *ca2cal1 and ca2cal2* show growth retardation in normal air.
Plants of the indicated genotypes were grown under ambient conditions as described in Experimental procedures for 4 weeks and then measured and photographed.
(a) Phenotype of 4-week-old plants of the indicated genotypes. The phenotype for *cal1* is similar to that for the *cal2* single mutant. Double mutants are consistently smaller.
(b) Leaf morphology of the fourth leaf of the same genotypes. Leaves of double mutants have a smaller leaf area.
(c) Maximum rosette radius of the same genotypes as in (a) and (b).
(d) Fresh weight was determined for entire rosettes of the indicated genotypes.
(e) Plants were then dried in an oven at 105°C for 24 h.
Asterisks indicate statistically significant differences compared with the WT (*$P \leq 0.05$).

type gene in the double mutant background should reverse the observed phenotype. In order to complement the *ca2cal2* double mutant, plants were transformed with a construct containing the entire genomic sequence of *CA2*. As shown in Figure 2(a,b), the complemented plants recovered WT phenotypic characteristics and *CA2* transcript levels.

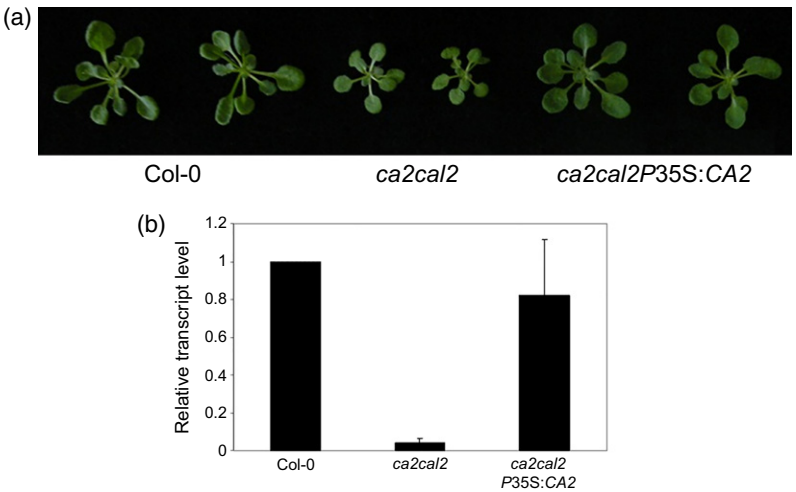

Figure 2. The *CA2* genomic sequence complements *ca2cal2* plants.
ca2cal2 mutant plants were transformed with the entire genomic sequence corresponding to the *CA2* gene (At1g47260) in a vector conferring resistance to hygromicin.
(a) T_3 transgenic plants of the indicated genotypes were planted onto MS medium under ambient conditions using Col–0 as a control.
(b) Transcript levels of the *CA2* gene are consistent with rescued phenotypes.

The phenotype of *ca* double mutants was rescued by growing plants in a high-CO_2 atmosphere

We recently postulated that the CA domain may be laterally involved in carbon recycling in the context of photorespiration and one-carbon metabolism (Braun and Zabaleta, 2007; Zabaleta *et al.*, 2012). Therefore, plants were germinated and grown for 4 weeks in a high-CO_2 atmosphere (2000 $\pm$ 200 ppm), which dramatically reduces photorespiration (Maier *et al.*, 2012). All other conditions remained unchanged. All single mutants, including *cal1*, behaved as the WT. The growth retardation seen in normal air for *ca2cal1* or *ca2cal2* double mutants (Figure 1a) was fully rescued under non-photorespiratory conditions (i.e. elevated CO_2, Figure 3a). The leaves of all genotypes show a narrow shape, a feature that is characteristic of plants growing under high-CO_2 conditions. No differences were observed between mutants and WT plants (Figure 3b,c). This phenotype of the *ca* double mutants (small size in normal air and WT behavior under high-CO_2 conditions) is reminiscent of previously described mutants showing a weak photorespiratory phenotype; this has been named the class III photorespiratory phenotype (Timm *et al.*, 2012). These results thus suggest that the CA domain has a function linked to photorespiration.

ca double mutants show similar oxygen consumption to *ca2* single mutants

Previous work indicated that *ca2* single mutants contain 80% less CI than WT plants (Perales *et al.*, 2005; Meyer *et al.*, 2011; Li *et al.*, 2013), and that oxygen consumption of *ca2* green leaves and cell suspensions growing in the dark is approximately 50% of that found in WT leaves or cells, respectively (Perales *et al.*, 2005). This low level of oxygen consumption is similar to that obtained for WT leaves pretreated with rotenone, the specific inhibitor of CI, leading to the conclusion that the main entry of electrons in the *ca2* mutant occurs through complex II and/or the alternative respiration pathway (Perales *et al.*, 2005; Villarreal *et al.*, 2009). To determine whether severe impairments in mitochondrial respiration are a cause of the phenotype observed in the double mutant plants, *ca2cal1* and *ca2cal2*, oxygen consumption normalized by fresh weight was measured in green leaves of all single and double mutants grown in normal air. We found that both *ca2cal1* and *ca2cal2* double mutants have the same respiratory rate as the *ca2* single mutant (Figure 4), indicating that the observed phenotype cannot be attributed to defects in respiration.

Complex I levels are similar in all *ca2* containing mutants

All double mutants that we obtained are knockouts for *CA2*, a mutation that decreases the amount of CI (Perales *et al.*, 2005; Meyer *et al.*, 2011). To determine whether the second mutation further reduces CI levels in the double mutants in comparison with known *ca2* single mutants, mitochondria of *ca2cal2* plants were isolated and CI levels and activity were analyzed. As shown in Figure 5 and Figure S2, CI levels and NADH dehydrogenase activity are strikingly similar between *ca2cal2* and *ca2* mutants.

In order to assess whether the second mutation affects pyrimidine nucleotide recycling, we measured the NADH/NAD^+ ratio in whole leaves and mitochondria of WT and all *ca2* containing mutants. As shown in Figure S3, the NADH/NAD^+ ratio is lower in WT than in any mutant. This result is consistent with our finding that all mutants containing low amounts of CI oxidize less NADH. However, there were no significant differences between single *ca2* and double *ca2cal* lines with respect to the NADH/NAD^+ ratio. We therefore conclude that similar amounts of CI contribute equally to NADH recycling.

This result, together with the oxygen consumption and NADH dehydrogenase activity results, strongly suggests that defects in respiration or NADH content are not the

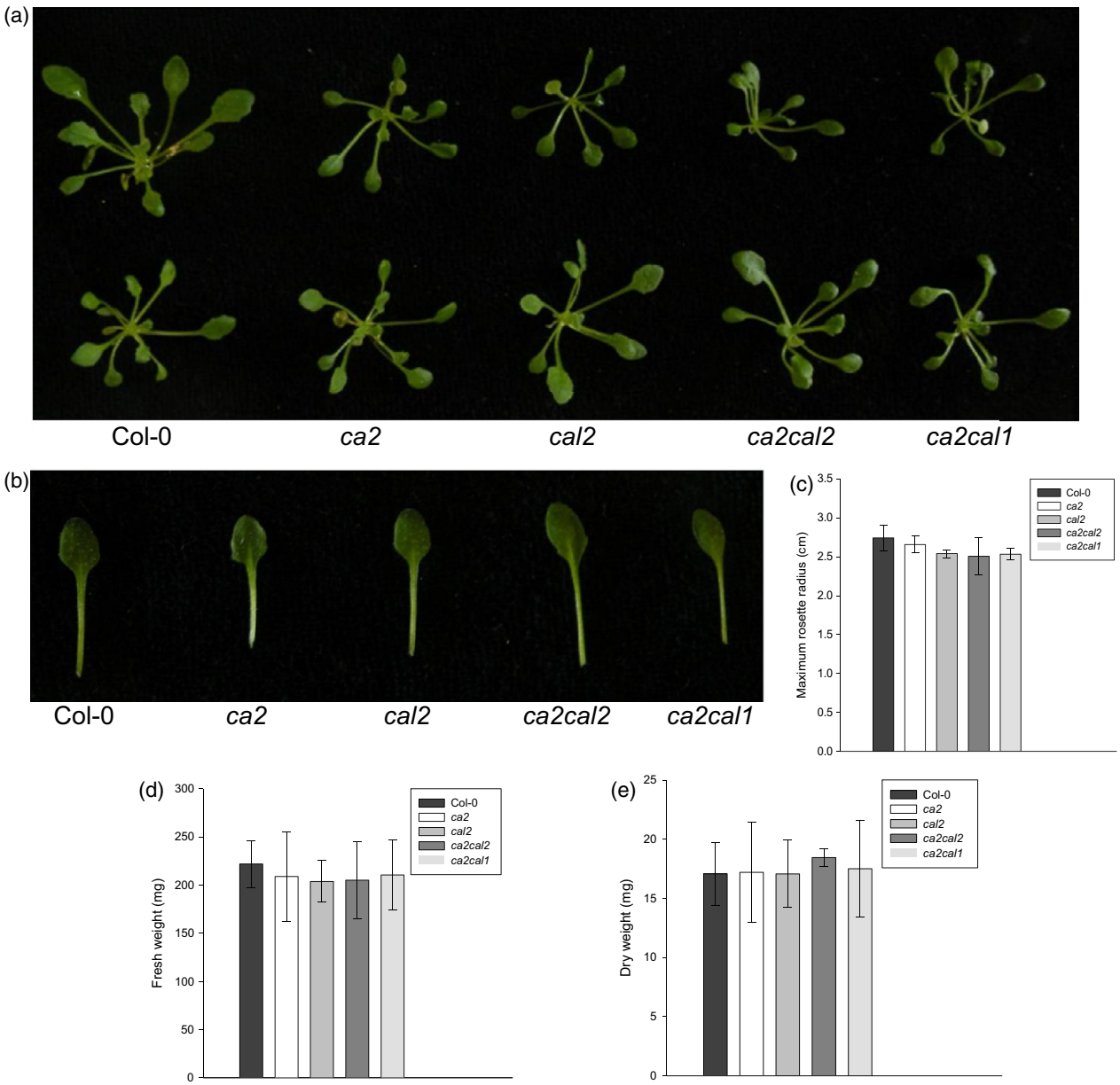

Figure 3. The phenotype of *ca2cal1* and *ca2cal2* is rescued under high-CO_2 conditions.
Plants of the indicated genotypes were grown under high-CO_2 conditions (2000 ppm) as described in Experimental procedures for 4 weeks and then measured and photographed.
(a) Phenotype of 4-week-old plants of the indicated genotypes. The phenotype for *cal1* is similar to that for the *cal2* single mutant. No growth differences were observed.
(b) Leaf morphology of the fourth leaf of the same genotypes.
(c) Maximum rosette radius of the same genotypes as in (a) and (b).
(d) Fresh weight was determined for entire rosettes of the indicated genotypes.
(e) Plants were then dried in an oven at 105°C for 24 h.
No statistically significant differences were observed.

cause of the growth retardation phenotype observed in the double mutants under photorespiratory conditions.

ca double mutants are impaired in photosynthesis

In order to analyze the carbon assimilation rate, gas exchange experiments were performed using WT, *ca* single and double mutants. The normal carbon assimilation rate (measured at a photon flux density of 250 μmol m^{-2} sec^{-1} and 380 ppm of CO_2) is approximately 12 μmol CO_2 m^{-2} sec^{-1} in the WT (100%) as well as in the single mutants (Figure 6), indicating that neither reduction of CAL2 nor lack of CA2 alone affects photosynthesis. However, *ca2cal2*

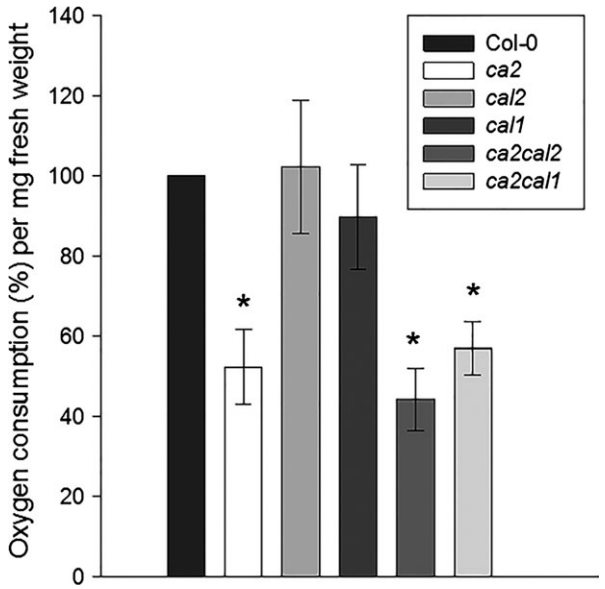

Figure 4. The *ca2* single mutant and the double mutants *ca2cal1* and *ca2cal2* show similar oxygen consumption profiles.
Plants of the indicated genotypes were grown for 4 weeks, and 200 mg of leaves were used for determination of oxygen consumption. Two technical and three biological replicates were used. Asterisks indicate statistically significant differences compared with the WT ($P \leq 0.001$).

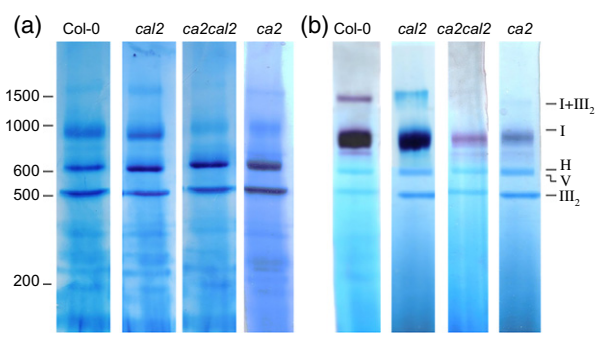

Figure 5. *ca2cal2* and *ca2* contain similar levels of CI.
Mitochondria were isolated from wild-type and the indicated mutant cell lines. Mitochondrial protein complexes were separated by one-dimensional blue native PAGE. Gels were either Coomassie-stained (a) or analysed for CI activity (b). The molecular masses of standard proteins are given on the left (in kDa), and the identities of protein complexes are shown on the right. $I+III_2$, supercomplex formed of complex I + dimeric complex III; I, complex I; H, HSP60 complex; V, ATP synthase complex; III_2, dimeric complex III.

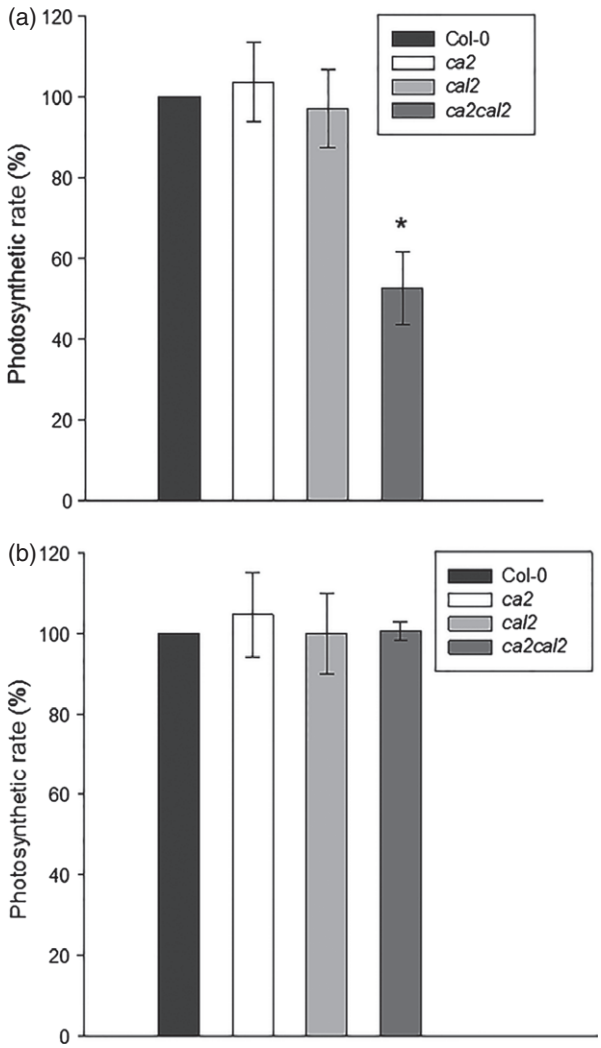

Figure 6. *ca2cal2* shows low levels of carbon assimilation.
Plants of the indicated genotypes were grown for 4 weeks under ambient (a) or elevated (b) CO_2, and at least two individual leaves for each plant were subjected to gas exchange determination using infrared gas analyzer. In the case of some small *ca2cal2* double mutant plants grown at normal atmosphere, more than one leaf per determination was needed due to their sizes. Two technical and three biological replicates were used. The asterisk indicates a statistically significant difference compared with the WT ($P \leq 0.001$).

double mutants show a carbon assimilation rate that is approximately 40% lower than that of the WT and single mutants (Figure 6a). Furthermore, double mutants show a slight decrease in photosystem II activity, and consequently a tendency for increased non-photochemical quenching (Figure S4a,b). These differences arise from lower amounts of the final electron acceptor ($NADP^+$) (Bartoli *et al.*, 2005).

Differences in CO_2 assimilation may be due to variations in stomatal conductance and/or stomatal index. As these parameters are similar in WT, *ca2* single and *ca2cal1* and *ca2cal2* mutants (Figure S5a,b), we conclude that, under ambient conditions, the *ca2cal* double mutants are impaired in CO_2 assimilation. In addition, these results strongly suggest that the growth retardation observed in all *ca* double mutants is most likely due to a low carbon assimilation rate. As *ca* double mutants are rescued under high CO_2, carbon assimilation was measured under these conditions. We found that, under high–CO_2 conditions, the carbon assimilation rate of all mutant lines was similar to

that of the WT (Figure 6b). This result strengthens the hypothesis that, under non-photorespiratory conditions, all genotypes present similar growth because carbon assimilation is not affected. It was therefore concluded that the greater impairment of CA domain function in the double mutants affects the extent of carbon fixation by Rubisco in normal air.

Transcript levels of specific CA subunits depend on the CO_2 level in air

In order to study the regulation of *CA* genes in relation to the atmospheric CO_2 concentration, WT plants were grown in normal air (380 $\pm$ 50 ppm CO_2) or under high-CO_2 conditions (700 and 2000 $\pm$ 200 ppm CO_2), and transcript levels of all CA genes were analyzed by quantitative RT–PCR. As shown in Figure 7, the steady-state level of *CA2* and *CAL1* transcripts dramatically decreased at high CO_2. The transcript levels of *CA1* and *CAL2* are also down-regulated, although to a lesser extent, under non-photorespiratory conditions. These results reveal that specific trimers containing CA2 may be required under normal air but may be dispensable under non-photorespiratory conditions, as has been demonstrated for other genes related to photorespiration in many organisms (Joët *et al.*, 2001). In contrast, transcript levels of other CI subunits are up-regulated under high CO_2 conditions (Figure S6).

Metabolic profiling of *ca2cal2* double mutants suggests a metabolic imbalance in photorespiration

In order to obtain a deeper understanding of the role of the CA domain of respiratory CI, we determined the profile of several metabolites in rosettes of WT, *ca2*, *cal2* and *ca2cal2* double mutants growing under short-day photorespiratory conditions (Table S1). The *ca2cal2* mutants showed a similar general response to the *ca2* mutant, with some additional changes. For all measured metabolites, glycine was the most altered in the *ca2cal2* plants compared with WT (Table 1, Figure 6, Figure S7 and Table S2). The *ca2cal2* mutant exhibited 2.8-fold higher glycine contents than the WT, while the single mutants *ca2* and *cal2* showed 2.0- and 1.3-fold higher glycine contents than the WT, respectively (Table 1 and Table S2). The amount of glycerate, a metabolite also related to photorespiration, is increased in the *ca2cal2* and *cal2* mutants (Table 1 and Table S2). The level of glycolate is slightly decreased in *ca2cal2*.

Thus, accumulation of glycine is the most significant difference in the metabolic profile of double mutants compared to that of WT plants. To corroborate this result and to test whether this accumulation is dependent on photorespiratory activity, the glycine content of rosette leaves was measured by HPLC at the end of the day (after 12 h illumination) and at the end of the night. As shown in Figure 8, glycine levels increased from 2.05 μmol g^{-1} fresh weight at the end of the night (considered as 100%) to 2.5 μmol g^{-1} fresh weight (122%) at the end of the day (after 12 h of illumination) in the WT. These results are similar to those reported by Hoffmann *et al.* (2013). Interestingly, at the end of the day, the *ca2cal2* and *ca2cal1* double mutants exhibited 4–6 times higher contents of glycine (500–700%, approximately 10–14 μmol g^{-1} fresh weight) compared with the WT (Figure 8). Glycine levels were also higher at

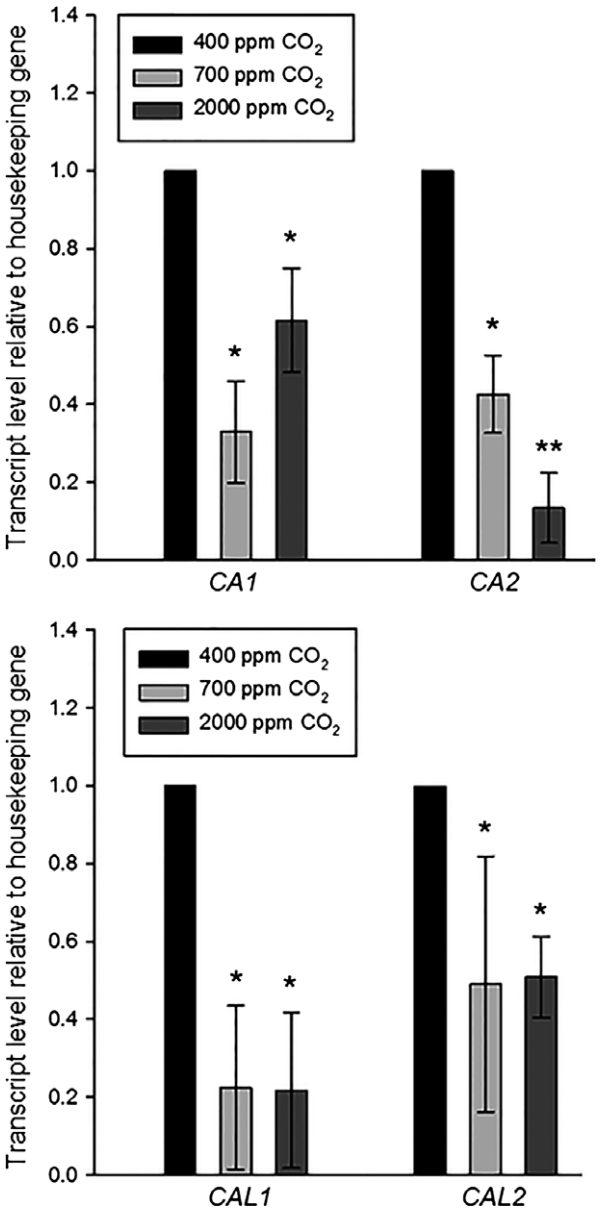

Figure 7. Transcript levels of *CA* genes are reduced at high CO_2 atmosphere.
WT plants were grown under various atmospheric conditions (400, 700 and 2000 ppm of CO_2) as described in Experimental procedures for 4 weeks. RNA was then extracted and quantitative PCR assays using specific primers for each gene were performed. Values are normalized using *UBQ5* and *ACT2* as housekeeping genes. Two technical and three biological replicates were used. Asterisks indicate statistically significant differences compared with the WT (*$P \leq 0.05$; **$P \leq 0.001$).

Table 1 Photorespiratory metabolite levels of indicated genotypes

	WT	*ca2*	*cal2*	*ca2cal2*
Glycerate	0.25 ± 0.02	0.26 ± 0.03	**0.35 ± 0.01**	**0.34 ± 0.02**
Glycine	2.14 ± 0.04	**4.29 ± 0.32**	**2.84 ± 0.15**	**6.05 ± 0.21**
Glycolate	0.39 ± 0.02	0.38 ± 0.01	0.44 ± 0.04	**0.34 ± 0.01**
Serine	0.31 ± 0.02	0.35 ± 0.04	0.26 ± 0.03	0.31 ± 0.01

Photorespiratory metabolite levels (relative to the internal standard molecule) were measured by GC-MS of whole rosette leaves harvested after 6 h in the light (130 μmol quanta m^{-2} sec^{-1}) from plants grown in air at 380 ppm CO_2. The values are normalized per area, and are means ± SE of four or five biological samples. Those shown in bold are statistically significantly different from WT values (Student's *t* test, $P < 0.05$).

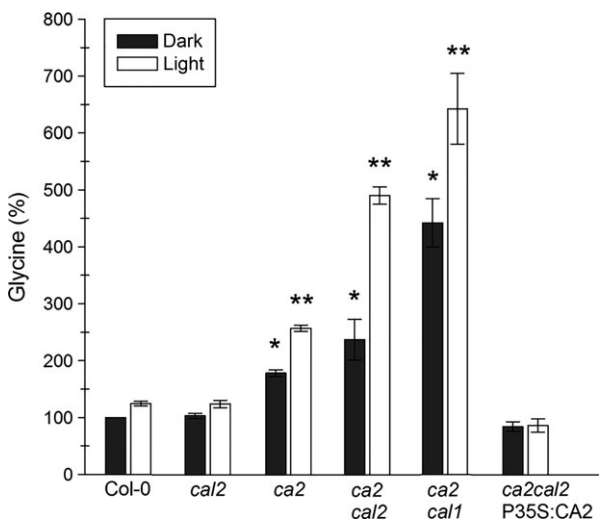

Figure 8. The double mutants *ca2cal1* and *ca2cal2* show increased levels of glycine.
Plants of the indicated genotypes were grown under ambient conditions for 4 weeks, and free amino acids were extracted from leaves as described in Experimental procedures. Glycine content was determined by HPLC. Black bars represent the end of the night, and white bars represent the end of the day (12 h of illumination). Two technical and two biological replicates were used. Asterisks indicate statistically significant differences compared with Col-0 at the end of the night or the end of the day (*$P \leq 0.05$; **$P \leq 0.001$).

the end of the night, but to a lesser extent. The greater differences in glycine contents between the WT and double mutant plants during the light phase indicate that glycine accumulation may be associated with light-dependent processes. In complemented lines expressing the transgene *CA2* in the *ca2cal2* background, glycine content reverted to WT levels, indicating that the observed imbalance was due to the double mutation in the CA domain.

ca double mutants show imbalanced levels of transcripts encoding photorespiratory enzymes and increased ROS levels

Higher glycine levels may be due to an imbalance in photorespiration. The oxygenase activity of Rubisco produces 2–PG, which is dephosphorylated into glycolate, which is transported to the peroxisome for further catabolism to glycine through GOX and GGAT. Glycine is then further transported to the mitochondria, where one molecule is decarboxylated by GDC and combined with a second glycine by SHMT to produce one molecule of serine, CO_2, NH_4 and NADH. The observed glycine accumulation may be due in part to (i) an increased rate of the oxygenation reaction by Rubisco, and/or (ii) increased production of glycine through GOX and GGAT enzymes, and/or (iii) partial inhibition of GDC and SHMT enzymes. In order to investigate the expression of these enzymes in the various genotypes, the transcript levels of the genes encoding the photorespiratory proteins GOX1, GOX2, GGAT, the P1 subunit of GDC (the actual decarboxylating subunit), SHMT1 and Glycerate 3-kinase (GLYK) were evaluated by quantitative RT–PCR. Interestingly, the results reveal that the transcript levels of *GOX1*, *GOX2*, *GGAT* and *GLYK* are increased in both *ca2* and *ca2cal* double mutants, while the transcript levels for GDC and SHMT are moderately reduced with respect to the WT (Figure S8).

In addition, it is known that GDC is sensitive to attack by ROS (Taylor *et al.*, 2002; Palmieri *et al.*, 2010; Hoffmann *et al.*, 2013). Thus, the levels of hydrogen peroxide and superoxide were evaluated in leaves of WT and *ca* single and double mutants. As shown in Figure 9, *ca2* single mutants show moderately enhanced levels of ROS, while *ca2cal* mutants show further increased levels of both hydrogen peroxide and superoxide.

As glycine levels are increased and the P1 subunit of GDC is slightly reduced in the *ca* double mutants, we determined the extractable GDC activity in plants of the various genotypes (Igamberdiev *et al.*, 1997; Hoffmann *et al.*, 2013). Surprisingly, in the double *ca* mutants, GDC activity is approximately 3.5-fold increased compared with the WT and the single *ca2* mutant (Figure 10), suggesting

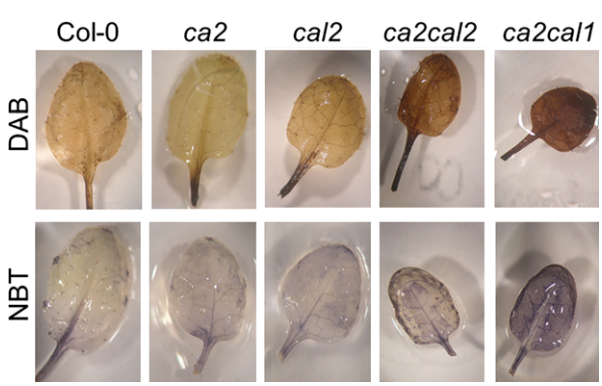

Figure 9. Leaves of *ca2cal1* and *ca2cal2* double mutants exhibited increased ROS levels.
Fully expanded leaves from plants of the indicated genotypes were subjected to staining with diaminobenzidine tetrahydrochloride (a) and nitroblue tetrazolium (b) as indicated in Experimental procedures to determine peroxide and superoxide levels, respectively.

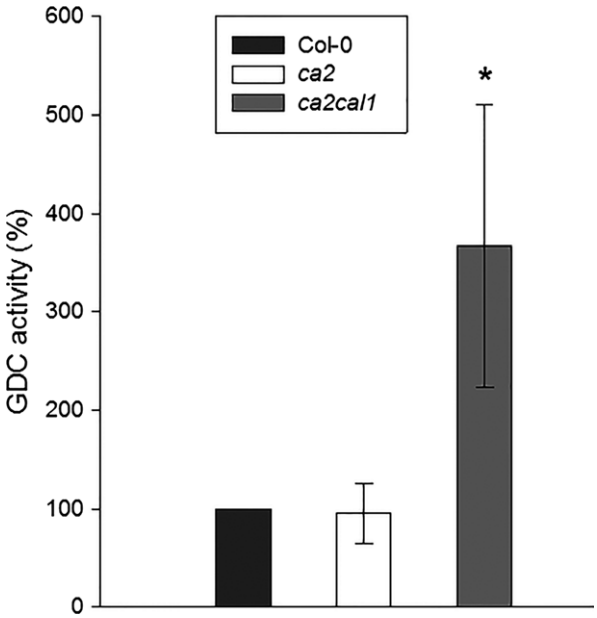

Figure 10. *ca2cal1* show increased glycine decarboxylase activity.
Crude mitochondrial extract were obtained from plants grown in ambient conditions as described in Experimental procedures. [^{14}C]-glycine was added to a reaction tube, and evolved [^{14}C]-CO_2 was trapped in a small tube containing potassium hydroxide (KOH) as indicated. Radioactivity was quantified by scintillation counting. Asterisks indicate statistically significant differences compared with WT ($P \leq 0.05$).

specific induction of the glycine decarboxylation reaction in these plants.

DISCUSSION

Here we show that double mutants of the CA subunits CA2 and CAL (*ca2cal1* and *ca2cal2*) have a phenotype characterized by small leaves and growth retardation. This phenotype is rescued by growing the plants under high-CO_2 atmosphere (non-photorespiratory conditions), and is thus compatible with a class III photorespiratory phenotype. Growth experiments were performed at 100 (micromol of quanta) μE m^2 s^{-1}. It remains to be established whether the *ca2cal* phenotype is completely rescued by high CO_2 in the presence of increased light intensities. Furthermore, carbon assimilation is affected, and glycine accumulates to high levels in the light, suggesting a photorespiratory imbalance. In addition, we found that expression of the *CA* genes is down-regulated under non-photorespiratory conditions in WT plants. Altogether, these results suggest that the CA domain of respiratory CI may be functionally linked to photorespiration.

Respiratory features of *ca* double mutants are indistinguishable from those of *ca2* single mutants

Even though the single mutant *ca2* does not show any visible altered phenotype, it contains 80% less CI than WT plants (Figure 5) (Perales *et al.*, 2005; Meyer *et al.*, 2011; Li *et al.*, 2013). The phenotype observed in the *ca2cal* mutants *ca2cal1* and *ca2cal2* may be explained by a reduction in CI levels to a level below that in *ca2* single mutants. However, respiration and proteomic experiments indicate that oxygen consumption, CI level, NADH dehydrogenase activity and NADH/NAD^+ ratio are similar in the *ca2* single mutant and in *ca2cal2* double mutants. These results indicate that the observed phenotype cannot be attributed to impaired respiration or NADH recycling. Furthermore, the results suggest that, in the *ca2cal* mutants, which express only three of five CA subunits, the CA domain may assemble at the same level and stability as in the *ca2* single mutant (expressing four subunits), and that the CAL1 or CAL2 subunits separately may not be essential for this process.

The phenotype observed in the *ca2cal* double mutant plants is similar to that observed previously by Wang *et al.* (2012) for *cal1cal2* RNAi plants with respect to plant size. However, while these silenced plants showed a late-germination phenotype, the *ca2cal* double mutants do not show any delay in germination under normal air conditions. Moreover, growth retardation in the *ca2cal* double mutants is only observed from the 10th day of growth, when photosynthesis is fully active. This differential behavior indicates that distinct processes may be affected in both cases, i.e. by silencing both *CAL* genes or by mutating *CA2* and a second *CA* family member, especially a *CAL* gene. Indeed, double knockout *cal1cal2* mutants showed an embryo-lethal phenotype (Wang *et al.*, 2012), while *ca2cal1* double knockouts germinate normally. These divergences may also account for the different behavior under high-CO_2 atmosphere.

Less CA activity is required in wild-type plants under high-CO_2 atmosphere

Under non-photorespiratory conditions, the oxygenase activity of Rubisco is suppressed (Maier *et al.*, 2012; Florian *et al.*, 2013), and, consequently, the photorespiratory pathway is dispensable. In several organisms ranging from algae to plants, transcription of genes encoding proteins involved in this pathway is much reduced under these conditions (Price, 2011; Timm *et al.*, 2012; this work). Consistent with this conclusion, we found that the transcript levels of *CA2*, *CA1* and *CAL* are reduced in Arabidopsis plants grown under high CO_2 (Figure 7), supporting the idea that the proteins encoded by these genes are linked to photorespiration.

However, other genes encoding CI subunits show increased transcript levels under an elevated CO_2 atmosphere (Figure S6). Consistently, it was reported that many transcripts of CI subunits increased under a moderately high CO_2 atmosphere (500 ppm) in soybean (*Glycine max*) (Leakey *et al.*, 2009). Unfortunately, they did not provide information on transcripts encoding the CI-integrated CA

subunits. Flux data combining transcriptomic and physiological approaches in Arabidopsis provided evidence of increased capacity for respiration of plants grown under moderately elevated CO_2 conditions, which should increase the ability to use greater amounts of carbohydrates (Watanabe *et al.*, 2014). However, there were no significant differences in the maximal respiratory activity of each respiratory enzyme between the two CO_2 conditions. Thus, although the respiratory capacity of plants was higher under elevated CO_2 than under ambient CO_2, there was no difference in the maximal enzymatic activities between the two CO_2 atmospheres. Therefore, the increased transcript levels of genes encoding respiratory enzymes under elevated CO_2 did not result in enhanced enzymatic activities of the corresponding proteins (Watanabe *et al.*, 2014). As it has recently been reported that CA2 is essential for CI assembly (Meyer *et al.*, 2011; Braun *et al.*, 2014), the lower level of *CA2* transcript under high-CO_2 conditions may affect CI assembly unless a similar protein replaces CA2. The fact that transcript levels of other CI subunits are increased or not changed suggests an alteration in the CI assembly pathway at high CO_2 or the existence of compensatory mechanisms to adjust protein levels under different atmospheres. These hypotheses remain to be tested.

ca double mutants produce high levels of ROS

The *ca* double mutants show increased levels of ROS and decreased carbon assimilation. Decreased carbon assimilation may be ascribed to a lower amount of mitochondrial CI with a CA domain showing reduction of bicarbonate export in these mutants. If a lower concentration of CO_2 is present in the vicinity of Rubisco, the oxygenation activity is augmented, triggering an increase in the rates of photorespiration. The GOX reaction in the peroxisomes produces H_2O_2, and the plant capacity to scavenge ROS may be overwhelmed. In addition, superoxide or H_2O_2 production by mitochondrial CI, which is dependent on the ratio of NADH to NAD^+, is inhibited by increasing NAD^+ (Hirst *et al.*, 2008). When the amount of CI is reduced, the ratio of NADH to NAD^+ is elevated (Figure S3), even in the presence of rotenone-insensitive NADH dehydrogenases, because of the reduction of total NADH dehydrogenase activity. We thus hypothesize that the reduced CI present in all *ca* containing mutants may trigger mitochondrial superoxide production and indirectly increase H_2O_2 levels.

Independent *ca* double mutants show a photorespiratory phenotype

During the photorespiratory cycle, glycine is produced in the peroxisomes by GGAT and transported into the mitochondria. Inside mitochondria, GDC and SHMT catalyze the conversion of two molecules of glycine into one molecule of serine, CO_2, ammonium and NADH (Maurino and Peterhänsel, 2010; Florian *et al.*, 2013). The *ca* double mutants, *ca2cal1* and *ca2cal2*, accumulate glycine to high amounts under photorespiratory conditions (Figure 8), and this is the main change observed in metabolic profiling (Figure S7 and Table S2). Moreover, glycine accumulation is dependent on light, which strengthens the idea of a photorespiratory imbalance (Figure 8). The lower glycine contents observed in the *ca2cal* mutants during the night compared with the day indicates that the mutant plants are capable of glycine degradation, and that glycine accumulation is dependent on light. The reversion of glycine content observed in the complemented lines suggests that the photorespiratory imbalance is due to the double mutation in two subunits of the CA domain.

If the modified CA domain in the *ca* double mutants impairs bicarbonate export from mitochondria to chloroplasts, then accumulation of CO_2 (in equilibrium with bicarbonate) in the mitochondrial matrix is expected, where it probably partially inhibits GDC activity. Even though there is little information in plants about the competitive inhibition of GDC by CO_2, chicken P–protein has been shown to be strongly inhibited by CO_2, while bicarbonate has no effect (Fujiwara and Motokawa, 1983; Bykova *et al.*, 2014). Experiments with CA inhibitors such as ethoxylamide indicate that the inter-conversion of CO_2 and bicarbonate is particularly important for GDC operation (Bykova *et al.*, 2014). This suggests that CA (complex I γ–CAs and/or matrix β–CA) may play a role in facilitating the GDC reaction by stimulating inter-conversion of CO_2 and $^-HCO_3$. The mitochondrial CAs may serve as buffers that help to remove the product (CO_2) from the GDC active site, thus facilitating glycine conversion to maintain a photorespiratory flux.

It has also been suggested that CAs may play a role in removal of ammonia produced by the GDC reaction during photorespiration (Bykova *et al.*, 2014). In addition, inhibition of CI, as occurs in all *ca2* mutants, generates an over-reduction of the complex. Consequently, superoxides and H_2O_2 are produced, contributing to a high oxidative environment that has been reported to inhibit GDC activity via *S*–nitrosylation/*S*–glutathionylation (Palmieri *et al.*, 2010). Despite these putative inhibiting factors, a glycine decarboxylating activity higher than WT was observed in the *ca* double mutants, suggesting that synthesis of glycine via GOX/GGAT is high. In line with this, we found enhanced transcript levels of genes encoding these enzymes in the *ca* double mutants.

Thus, several results were obtained that may explain the observed glycine accumulation in the *ca* double mutants: (i) enhanced transcript levels of genes encoding GOX and GGAT that presumably lead to production of large amounts of glycine in the *ca* double mutants, (ii) elevated ROS production in the *ca* double mutants due to higher photorespiratory flux and over-reduced CI, (iii) enhance-

ment of the photorespiratory pathway through activation of GOX and GGAT enzymes by this elevated ROS, as observed in the *ca2 cal* mutants, (iv) higher GDC activity in the *ca2 cal* mutants, which may be not sufficient to allow catabolism of the increased amounts of glycine produced, and (v) a presumably local accumulation of bicarbonate/CO_2 (one of the products of respiration/photorespiration) in the mitochondrial matrix of *ca2 cal* mutants. These effects contribute to a situation of metabolic imbalance, with high photorespiratory rates that account for the observed glycine accumulation.

CONCLUSIONS

In this work, using a combination of insertional mutants in *CA* genes, we have shown that lack of two CA/CAL proteins of the CA domain causes a photorespiratory imbalance characterized by accumulation of glycine and a reduction of carbon assimilation by Rubisco. This leads to reduced plant growth under normal air conditions that may be rescued by growing the plants in a non-photorespiratory environment. A dysfunctional CA domain most likely results in enhancement of flux through the photorespiratory pathway. Altogether, these results suggest that the CA domain of the plant respiratory CI may represent a missing component of the photorespiratory pathway as predicted previously (Raven, 2001; Riazunnisa *et al.*, 2006), which contributes to sustaining photosynthesis.

Our data provide experimental support with respect to the proposed basal carbon recycling pathway in plants (Raven, 2001; Braun and Zabaleta, 2007, Zabaleta *et al.*, 2012), and strengthen the evidence for the predicted chloroplast/mitochondria cross-talk.

EXPERIMENTAL PROCEDURES

Plant material and growth conditions

All studies were performed using *Arabidopsis thaliana* wild-type (WT) plants of ecotype Columbia–0 and T–DNA insertion mutants of CA2 (*ca2*, SALK_010194), CAL1 (*cal1*, SALK_072274) and CAL2 (*cal2*, CS810918) as described previously (Perales *et al.*, 2005). Prior to germination, seeds were incubated for 2 days in the dark at 4°C on standardized soil (soil-vermiculite-perlite). Plants were grown at 22°C and 100 μE m^2 sec^{-1} light under a 12 h light/12 h dark regime either at ambient CO_2 levels (380 ppm CO_2) or at high CO_2 levels (2000 ppm CO_2; Maier *et al.*, 2012) in plant climate chambers.

Seeds were sterilized by incubation 15 min. in 20% v/v sodium hypochlorite, washed with sterile water at RT, and plated on Murashige and Skoog plates containing 50 μg ml^{-1} kanamycin and/or 15 μg ml^{-1} sulfadiazine. Resistant (green) seedlings were then transferred onto soil and grown under the conditions described above.

Stomatal index

Plants were grown under ambient conditions. Stomatal indices were determined in individual leaves as described previously (Casson *et al.*, 2009; Hu *et al.*, 2010).The stomatal index is the ratio of the number of stomata in a given area divided by the total number of stomata and other epidermal cells in that same area.

Molecular methods

Genomic DNA was extracted from rosette leaves as previously described (Martin *et al.*, 2013). The genomic sequence of *CA2* (At1g47260) was amplified by PCR using forward primer 5′-CACCGGACTATTTCCGGATTTAGGC-3′ and reverse primer 5′-GAAGATTAATCCAACTTTG-3′. The amplicon was cloned into pENTR/TOPO (Invitrogen; http://www.lifetechnologies.com/ar/es/home/brands/invitrogen.html), and the sequence was verified. The resulting plasmid (pENTR-gCA2) was subjected to the LR reaction using destination vector V032pH7FWG2 (Grefen *et al.*, 2010). For genotyping, genomic PCR was performed using the primers listed in Table S3. Total RNA was extracted using TriZOL (Invitrogen) and used for quantitative PCR using Power SYBR PCR mix and a StepOne machine (Applied Biosystems; http://www.lifetechnologies.com/ar/es/home/brands/applied-biosystems.html). Values were normalized against the *UBQ5* and *ACT2* housekeeping genes. The primers used are listed in Table S3. Western blotting was performed as previously described using anti-CA2 antiserum (Perales *et al.*, 2005).

Cell suspension cultures

Arabidopsis suspension cultures were established from WT, *ca2*, *cal2* and *ca2cal2* Arabidopsis lines growing in the dark as described by May and Leaver (1993) and Perales *et al.* (2005). Cells were transferred once a week into fresh suspension cell medium. The growth rates of the suspension cell cultures were determined by weight determinations.

Transformation of *Agrobacterium tumefaciens* and Arabidopsis

Vectors for complementation of *ca* double mutants were introduced into *Agrobacterium* strain GV3101 by electroporation. Transformation into *ca* double mutants was performed by the floral-dip method (Clough and Bent, 1998). Transformants were selected based on their ability to survive on Murashige and Skoog medium containing 15 mg L^{-1} hygromycin. Resistant seedlings (green with true leaves) were then transferred to soil and grown under the conditions described above.

Oxygen consumption

Oxygen consumption of adult leaves was analyzed using a Clark-type oxygen electrode with a reaction chamber volume of 2 ml (Oxygraph, Hansatech; http://hansatech-instruments.com/) for 10 min. At least three replicates were used for each genotype. Detached leaves were pre-incubated for 2 h in the dark in a reaction buffer containing 0.3 M mannitol, 10 mM K_2HPO_4 (pH 7.2), 10 mM KCl and 5 mM $MgCl_2$ before measurements. Then entire leaves (approximately 200 mg) were introduced into the chamber and oxygen consumption was measured for 10 min. Values were normalized by fresh weight.

Mitochondria isolation and gel electrophoresis procedures

Isolation of mitochondria from cell suspensions and green Arabidopsis plants was performed as described previously (Perales *et al.*, 2005). 1D SDS–PAGE was performed as described by Schägger and von Jagow (1987), and 1D blue native PAGE as described by Wittig *et al.* (2006). Protein solubilization for blue

native PAGE was performed using digitonin at a concentration of 5 μg mg^{-1} mitochondrial protein as described by Eubel *et al.* (2003). Blue native separation of protein complexes was performed in gradient gels of 4.5–16% polyacrylamide.

Nucleotide pyridine determinations

$NADH/NAD^+$ contents were spectrophotometrically measured as described by Queval and Noctor (2007).

Carbon assimilation and fluorescence analyses

Photosynthetic parameters were measured using a CIRAS2 portable gas exchange system (PPSystems; www.ppsystems.com). Fully developed rosette leaves were first adjusted in the leaf chamber for 20 min. Measurements were performed at 25°C at a photosynthetic photon flux density of 250 μE m^{-2} sec^{-1}, 21% O_2 and ambient CO_2. Carbon assimilation rates were calculated using the CIRAS2 software.

For fluorescence analyses, plants of various genotypes were grown under 100 μE m^{-2} sec^{-1} light intensity for 5 weeks. Chlorophyll fluorescence parameters were then measured on well-illuminated leaves using an FMS2 fluorescence modulated system (Hansatech). Steady-state fluorescence parameters were measured, and F_v/F_m was measured after 30 min darkness. Fluorescence parameters were calculated as described by Bartoli *et al.* (2005). Non-photochemical quenching was calculated as $(F_m - F'_m)/F'_m$.

Metabolomic profiling

Plants were grown for 26 days under a 12 h light/12 h dark regime at 130 μE quanta m^2 sec^{-1} under ambient CO_2 (380 ppm) conditions. Whole-plant rosettes were harvested after 6 h in light, shock-frozen in liquid N_2, and stored at −80°C until extraction. Ground rosette material (approximately 50 mg) was extracted in methanol/chloroform/water (5:2:2) using ribitol for internal standardization as described by Lee and Fiehn (2008) and Fiehn (2007). Analysis of metabolites was performed by GC/MS using an accurate mass Q-TOF GC/MS system (Agilent 7890A GC system, Agilent Technologies; www.agilent.com). Metabolites were ionized in an EI source and detected using Waters GCT Premier TOF-MS. Data were analyzed with MassLynx and QuanLynx software (Waters GmbH, Eschborn, Germany; www.waters.com). Metabolites were identified and quantified by scanning the internal database. Integrated peak areas were normalized to determine relative metabolite levels per g fresh weight. Relative metabolite levels of four or five biological samples were averaged, and $\log_2$ fold changes in metabolite levels of WT versus mutant were color-coded and visualized as heatmaps.

Quantification of glycine by HPLC

For determination of glycine concentration, Arabidopsis leaf samples were harvested at the end of the day (after 12 h illumination) and at the end of the night (after 12 h darkness), and ground in liquid nitrogen using a mortar and pestle. Quantification of glycine by HPLC was performed as described by Jung *et al.* (2009) using 80% v/v ethanol as an extraction medium.

Glycine decarboxylase activity

Crude mitochondrial extracts of either WT or *ca* double mutants were used. Exogenous [1–^{14}C] glycine (Perkin-Elmer; www.perkinelmer.com) was applied at a concentration of 10 mM containing 0.1 MBq ml^{-1} radioactivity. Measurements were started by addition of mitochondrial extracts (100 μg of mitochondrial proteins) at 25°C. Evolved [^{14}C]-CO_2 was captured in small reaction tubes containing 100 μl of 5 M potassium hydroxide (KOH). The reaction was stopped after 30 min by injecting 100 μl of 2 M HCl into the reaction mixture with a syringe through the closed bromobutyl lid. The reaction mixtures were stored overnight to allow total absorption of radioactively labeled CO_2. The trapped radioactivity was quantified by scintillation counting using a Beckman LS 7000 liquid scintillation counter (Beckman Coulter; https://www.beckmancoulter.com). This method is modified from those described by Igamberdiev *et al.* (1997)and Hoffmann *et al.* (2013).

Detection of ROS

Histochemical staining was performed as previously described (Lee *et al.*, 2002; Reiser *et al.*, 2004) with the following modifications: to detect accumulation of superoxide, leaves from wild-type and *ca* double mutants were vacuum-infiltrated for 10 min with 0.1 mg ml^{-1} nitroblue tetrazolium in 25 mM HEPES buffer, pH 7.6. Leaf samples were left for 2 h at room temperature in the dark, and were subsequently de-stained by incubation at 60°C in 95% v/v ethanol for 30 min. The accumulation of H_2O_2 was visualized by vacuum infiltration of leaves in a solution containing 0.1 mg ml^{-1} diaminobenzidine tetrahydrochloride in 10 mM MES, pH 6.0, and 1 mM KOH. The control solution also contained 10 mM ascorbate. After infiltration, the leaves were incubated for 16 h in the dark, and de-stained by boiling in lactic acid/glycerol/ethanol (1:1:3) for 5–10 min.

ACKNOWLEDGMENTS

D.S. is a doctoral fellow of the Universidad Nacional de Mar del Plata, Argentina. J.P.C. is a doctoral fellow of the Consejo Nacional de Investigaciones Científicas y Técnicas (CONICET). M.V.M., C.B., G.C.P. and E.J.Z. are CONICET researchers. This research was funded by the Agencia Nacional de Promoción Científica y Técnica, the Deutscher Akademischer Austauschdienst, CONICET, the Howard Hughes Medical Institute and the Deutsche Forschungsgemeinschaft. We would like to thank Eduardo Tambussi (Instituto de Fisiología Vegetal, Universidad Nacional de La Plata/CONICET La Plata, cc 327, 1900 La Plata, Argentina) for help with gas exchange experiments, and helpful discussions and suggestions. We would like to thank Tabea Mettler (Institute of Plant Biochemistry, Heinrich-Heine-Universität) for helping with metabolome experiments. We thank Gustavo Uicich, Esteban Tocci and Facundo Rodriguez (Facultad de Ingeniería, Universidad Nacional de Mar del Plata, Argentina) for help setting up plant chambers with controlled atmospheres. We are grateful to Daniela Villamonte for excellent technical assistance with HPLC.

SUPPORTING INFORMATION

Additional Supporting Information may be found in the online version of this article.

Figure S1. Genotyping, transcript and protein levels in double mutants.

Figure S2. *ca2* containing double and single mutants show similar CI levels.

Figure S3. Effect of the CA subunit deficiency on the $NADH/NAD^+$ ratio.

Figure S4. Quantum yield of photosystem II and non-photochemical quenching.

Figure S5. Stomatal behavior in double mutants compared with single mutant and WT plants.

Figure S6. Transcript levels of genes encoding subunits of CI.

Figure S7. Heatmap for metabolomic profiling.

Figure S8. Transcript levels of photorespiratory genes.

Table S1. Metabolic profiling parameters.

Table S2. Metabolomic profiling of the indicated genotypes.

Table S3. Primers used for genotyping.

REFERENCES

Andrews, B., Carroll, J., Ding, S., Fearnley, I.M. and Walker, J.E. (2013) Assembly factors for the membrane arm of human complex I. *Proc. Natl Acad. Sci. USA*, **110**, 18934–18939.

Bartoli, C.G., Gomez, F., Gergoff, G., Guiamét, J.J. and Puntarulo, S. (2005) Up-regulation of the mitochondrial alternative oxidase pathway enhances photosynthetic electron transport under drought conditions. *J. Exp. Bot.*, **56**, 1269–1276.

Bauwe, H., Hagemann, M. and Fernie, A.R. (2010) Photorespiration: players, partners and origin. *Trends Plant Sci.*, **15**, 330–336.

Braun, H.P. and Zabaleta, E. (2007) Carbonic anhydrase subunits of the mitochondrial NADH dehydrogenase complex (complex I) in plants. *Physiol. Plant.*, **129**, 114–122.

Braun, H.P., Binder, S., Brennicke, A. *et al.* (2014) The life of plant mitochondrial complex I. *Mitochondrion*, **19**, 295–313.

Bridges, H.R., Fearnley, I.M. and Hirst, J. (2010) The subunit composition of mitochondrial NADH:ubiquinone oxidoreductase (complex I) from *Pichia pastoris*. *Mol. Cell Proteomics*, **9**, 2318–2326.

Bykova, N., Møller, I.M., Gardeströmc, P. and Igamberdiev, A.U. (2014) The function of glycine decarboxylase complex is optimized to maintain high photorespiratory flux via buffering of its reaction products. *Mitochondrion*, **19**, 357–364.

Cardol, P. (2011) Mitochondrial NADH:ubiquinone oxidoreductase (complex I) in eukaryotes: a highly conserved subunit composition highlighted by mining of protein databases. *Biochim. Biophys. Acta*, **1807**, 1390–1397.

Casson, S.A., Franklin, K.A., Gray, J.E., Grierson, C.S., Whitelam, G.C. and Hetherington, A.M. (2009) Phytochrome B and PIF4 regulate stomatal development in response to light quantity. *Curr. Biol.*, **19**, 229–234.

Clough, S.J. and Bent, A.F. (1998) Floral dip: a simplified method for *Agrobacterium*-mediated transformation of *Arabidopsis thaliana*. *Plant J.* **16**, 735–743.

Dudkina, N.V., Eubel, H., Keegstra, W., Boekema, E.J. and Braun, H.P. (2005) Structure of a mitochondrial supercomplex formed by respiratory-chain complexes I and III. *Proc. Natl Acad. Sci. USA*, **102**, 3225–3229.

Esser, C., Kuhn, A., Groth, G., Lercher, M.J. and Maurino, V.G. (2014) Parallel diversification of glycolate oxidase into long-chain 2-hydroxy acid oxidases in plants and animals. *Mol. Biol. Evol.*, **31**, 1089–1101.

Eubel, H., Jänsch, L. and Braun, H.P. (2003) New insights into the respiratory chain of plant mitochondria. Supercomplexes and a unique composition of complex II. *Plant Physiol.*, **133**, 274–286.

Fiehn, O. (2007) *Concepts in Plant Metabolomics*. Berlin: Springer. ISBN 978-1-4020-5608-6.

Florian, A., Araújo, W.L. and Fernie, A.R. (2013) New insights into photorespiration obtained from metabolomics. *Plant Biol. (Stuttg.)*, **15**, 656–666.

Friedrich, T. (1998) The NADH:ubiquinone oxidoreductase (complex I) from *Escherichia coli*. *Biochim. Biophys. Acta*, **1364**, 134–146.

Fujiwara, K. and Motokawa, Y. (1983) Mechanism of the glycine cleavage reaction. Steady-state kinetic-studies of the P-protein-catalyzed reaction. *J. Biol. Chem.*, **258**, 8156–8162.

Gawryluk, R.M. and Gray, M.W. (2010) Evidence for an early evolutionary emergence of gamma-type carbonic anhydrases as components of mitochondrial respiratory complex I. *BMC Evol. Biol.*, **10**, 176.

Gray, M.W. (2012) Mitochondrial evolution. *Cold Spring Harb. Perspect. Biol.*, **4**, a011403.

Grefen, C., Chen, Z., Honsbein, A., Donald, N., Hills, A. and Blatt, M.R. (2010) A novel motif essential for SNARE interaction with the K^+ channel KC1 and channel gating in Arabidopsis. *Plant Cell*, **22**, 3076–3092.

Heazlewood, J.L., Howell, K.A. and Millar, A.H. (2003) Mitochondrial complex I from Arabidopsis and rice: orthologs of mammalian and fungal components coupled with plant-specific subunits. *Biochim. Biophys. Acta*, **1604**, 159–169.

Hirst, J., King, M.S. and Pryde, K.R. (2008) The production of reactive oxygen species by complex I. *Biochem. Soc. Trans.*, **36**, 976–978.

Hoffmann, C., Plocharski, B., Haferkamp, I., Leroch, M., Ewald, R., Bauwe, H., Riemer, J., Herrmann, J.M. and Neuhaus, H.E. (2013) From endoplasmic reticulum to mitochondria: absence of the Arabidopsis ATP antiporter Endoplasmic Reticulum Adenylate Transporter1 perturbs photorespiration. *Plant Cell*, **25**, 2647–2660.

Hu, H., Boisson-Dernier, A., Israelsson-Nordström, M., Böhmer, M., Xue, S., Ries, A., Godoski, J., Kuhn, J.M. and Schroeder, J.I. (2010) Carbonic anhydrases are upstream regulators of CO_2-controlled stomatal movements in guard cells. *Nat. Cell Biol.*, **12**, 87–93.

Igamberdiev, A.U., Bykova, N.V. and Gardeström, P. (1997) Involvement of cyanide-resistant and rotenone-insensitive pathways of mitochondrial electron transport during oxidation of glycine in higher plants. *FEBS Lett.*, **412**, 265–269.

Joët, T., Cournac, L., Horvath, E.M., Medgyesy, P. and Peltier, G. (2001) Increased sensitivity of photosynthesis to antimycin A induced by inactivation of the chloroplast *ndhB* gene. Evidence for a participation of the NADH-dehydrogenase complex to cyclic electron flow around photosystem I. *Plant Physiol.*, **125**, 1919–1929.

Jung, B., Flörchinger, M., Kunz, H.H., Traub, M., Wartenberg, R., Jeblick, W., Neuhaus, H.E. and Möhlmann, T. (2009) Uridine-ribohydrolase is a key regulator in the uridine degradation pathway of Arabidopsis. *Plant Cell*, **21**, 876–891.

Klodmann, J., Sunderhaus, S., Nimtz, M., Jansch, L. and Braun, H.P. (2010) Internal architecture of mitochondrial complex I from *Arabidopsis thaliana*. *Plant Cell*, **22**, 797–810.

Leakey, A.D., Xu, F., Gillespie, K.M., McGrath, J.M., Ainsworth, E.A. and Ort, D.R. (2009) Genomic basis for stimulated respiration by plants growing under elevated carbon dioxide. *Proc. Natl Acad. Sci. USA*, **106**, 3597–3602.

Lee, D.Y. and Fiehn, O. (2008) High quality metabolomic data for *Chlamydomonas reinhardtii*. *Plant Methods*, **4**, 7.

Lee, B.H., Lee, H., Xiong, L. and Zhu, J.K. (2002) A mitochondrial complex I defect impairs cold-regulated nuclear gene expression. *Plant Cell*, **14**, 1235–1251.

Li, L., Nelson, C.J., Carrie, C., Gawryluk, R.M., Solheim, C., Gray, M.W., Whelan, J. and Millar, A.H. (2013) Subcomplexes of ancestral respiratory complex I subunits rapidly turn over *in vivo* as productive assembly intermediates in Arabidopsis. *J. Biol. Chem.*, **288**, 5707–5717.

Maier, A., Fahnenstich, H., von Caemmerer, S., Engqvist, M.K., Weber, A.P., Flügge, U.I. and Maurino, V.G. (2012) Transgenic introduction of a glycolate oxidative cycle into *A. thaliana* chloroplasts leads to growth improvement. *Front. Plant Sci.*, **3**, 38.

Martin, M.V., Villarreal, F., Miras, I., Navaza, A., Haouz, A., González-Lebrero, R.M., Kaufman, S.B. and Zabaleta, E. (2009) Recombinant plant gamma carbonic anhydrase homotrimers bind inorganic carbon. *FEBS Lett.*, **583**, 3425–3430.

Martin, M.V., Fiol, D.F., Sundaresan, V., Zabaleta, E. and Pagnussat, G.C. (2013) *oiwa*, a female gametophytic mutant impaired in a mitochondrial manganese-superoxide dismutase, reveals crucial roles for reactive oxygen species during embryo sac development and fertilization in Arabidopsis. *Plant Cell*, **25**, 1573–1591.

Maurino, V.G. and Peterhänsel, C. (2010) Photorespiration: current status and approaches for metabolic engineering. *Curr. Opin. Plant Biol.*, **13**, 249–256.

May, M.J. and Leaver, C.J. (1993) Oxidative stimulation of glutathione synthesis in *Arabidopsis thaliana* suspension cultures. *Plant Physiol.*, **103**, 621–627.

Meyer, E.H., Solheim, C., Tanz, S.K., Bonnard, G. and Millar, A.H. (2011) Insights into the composition and assembly of the membrane arm of plant complex I through analysis of subcomplexes in Arabidopsis mutant lines. *J. Biol. Chem.*, **286**, 26081–26092.

Palmieri, M.C., Lindermayr, C., Bauwe, H., Steinhauser, C. and Durner, J. (2010) Regulation of plant glycine decarboxylase by *S*-nitrosylation and glutathionylation. *Plant Physiol.*, **152**, 1514–1528.

Parisi, G., Perales, M., Fornasari, M. *et al.* (2004) Gamma carbonic anhydrases in plant mitochondria. *Plant Mol. Biol.*, **55**, 193–207.

Perales, M., Parisi, G., Fornasari, M.S. *et al.* (2004) Gamma carbonic anhydrase like complex interact with plant mitochondrial complex I. *Plant Mol. Biol.*, **56**, 947–957.

Perales, M., Eubel, H., Heinemeyer, J., Colaneri, A., Zabaleta, E. and Braun, H.P. (2005) Disruption of a nuclear gene encoding a mitochondrial gamma carbonic anhydrase reduces complex I and supercomplex I + III_2 levels and alters mitochondrial physiology in Arabidopsis. *J. Mol. Biol.*, **350**, 263–277.

Perez, E., Lapaille, M., Degand, H. *et al.* (2014) The mitochondrial respiratory chain of the secondary green alga *Euglena gracilis* shares many additional subunits with parasitic Trypanosomatidae. *Mitochondrion*, **19**, 338–349.

Peters, K., Belt, K. and Braun, H.P. (2013) 3D gel map of arabidopsis complex I. *Front. Plant Sci.*, **4**, 153.

Price, G.D. (2011) Inorganic carbon transporters of the cyanobacterial CO_2 concentrating mechanism. *Photosynth. Res.*, **109**, 33–45.

Queval, G. and Noctor, G. (2007) A plate reader method for the measurement of NAD, NADP, glutathione, and ascorbate in tissue extracts: application to redox profiling during Arabidopsis rosette development. *Anal. Biochem.*, **363**, 58–69.

Raven, R.A. (2001) A role for mitochondrial carbonic anhydrase in limiting CO_2 leakage from low CO_2-grown cells of *Chlamydomonas reinhardtii*. *Plant Cell Environ.*, **24**, 261–265.

Reiser, J., Linka, N., Lemke, L., Jeblick, W. and Neuhaus, H.E. (2004) Molecular physiological analysis of the two plastidic ATP/ADP transporters from *Arabidopsis thaliana*. *Plant Physiol.*, **136**, 3524–3536.

Riazunnisa, K., Padmavathi, L., Bauwe, H. and Raghavendra, A.S. (2006) Markedly low requirement of added CO_2 for photosynthesis by mesophyll protoplasts of pea (*Pisum sativum*): possible roles of photorespiratory CO_2 and carbonic anhydrase. *Physiol. Plant.*, **128**, 763–772.

Schägger, H. and von Jagow, G. (1987) Tricine-sodium dodecyl sulfate-polyacrylamide gel electrophoresis for the separation of proteins in the range from 1 to 100 kDa. *Anal. Biochem.*, **166**, 368–379.

Sunderhaus, S., Dudkina, N.V., Jänsch, L., Klodmann, J., Heinemeyer, J., Perales, M., Zabaleta, E., Boekema, E.J. and Braun, H.P. (2006) Carbonic anhydrase subunits form a matrix-exposed domain attached to the membrane arm of mitochondrial complex I in plants. *J. Biol. Chem.*, **281**, 6482–6488.

Taylor, N.L., Day, D.A. and Millar, A.H. (2002) Environmental stress causes oxidative damage to plant mitochondria leading to inhibition of glycine decarboxylase. *J. Biol. Chem.*, **277**, 42663–42668.

Timm, S., Mielewczik, M., Florian, A., Frankenbach, S., Dreissen, A., Hocken, N., Fernie, A.R., Walter, A. and Bauwe, H. (2012) High-to-low CO2 acclimation reveals plasticity of the photorespiratory pathway and indicates regulatory links to cellular metabolism of Arabidopsis. *PLoS ONE*, **7**, e42809.

Villarreal, F., Martín, V., Colaneri, A., González-Schain, N., Perales, M., Martín, M., Lombardo, C., Braun, H.P., Bartoli, C. and Zabaleta, E. (2009) Ectopic expression of mitochondrial gamma carbonic anhydrase 2 causes male sterility by anther indehiscence. *Plant Mol. Biol.*, **70**, 471–485.

Wang, Q., Fristedt, R., Yu, X., Chen, Z., Liu, H., Lee, Y., Guo, H., Merchant, S.S. and Lin, C. (2012) The γ–carbonic anhydrase subcomplex of mitochondrial complex I is essential for development and important for photomorphogenesis of Arabidopsis. *Plant Physiol.*, **160**, 1373–1383.

Watanabe, C.K., Sato, S., Yanagisawa, S., Uesono, Y., Terashima, I. and Noguchi, K. (2014) Effects of elevated CO_2 on levels of primary metabolites and transcripts of genes encoding respiratory enzymes and their diurnal patterns in *Arabidopsis thaliana*: possible relationships with respiratory rates. *Plant Cell Physiol.*, **55**, 341–357.

Wittig, I., Braun, H.P. and Schägger, H. (2006) Blue-Native PAGE. *Nat. Protoc.*, **1**, 418–428.

Zabaleta, E., Martin, M.V. and Braun, H.P. (2012) A basal Carbon Concentrating Mechanism in Plants? *Plant Sci.*, **187**, 94–104.

Zelitch, I., Schultes, N.P., Peterson, R.B., Brown, P. and Brutnell, T.P. (2009) High glycolate oxidase activity is required for survival of maize in normal air. *Plant Physiol.*, **149**, 195–204.